# Kinetic and Thermodynamic Studies of Crude Palm Oil Bleaching using Amansea Clay


## ABSTRACT

The effectiveness of the bleaching of crude palm oil was carried out using alkaline-activated Amansea clay. The clay sample was sun-dried, ground, sieved and activated with sodium hydroxide (NaOH) and Potassium hydroxide (KOH). The raw and alkaline-activated clay (AAMC) samples were characterized using Fourier transform infrared spectroscopy (FTIR), Scanning electron microscopy (SEM) and X-ray fluorescence (XRF) analyses. The dosage, temperature and contact time of the process were varied to observe the efficiency of the bleaching process. The results of the characterization indicated that the raw and activated clays were kaolinite and the clay changed significantly after activation. The bleaching efficiency improved with an increase in temperature and an increase in the mass of the adsorbent. The highest bleaching efficiency of 83.2% was obtained. The pseudo-second-order model best described the adsorption process at 100 oC. The Temkin isotherm model best fitted the experimental data when compared to the other isotherm models because it gave the highest $R^2$ values of >0.9 at all temperatures. The thermodynamics studies carried out from the experimental data indicated that the process was endothermic with an increase in randomness at the solid/liquid interface. The values of the enthalpy and entropy were evaluated as 6.193 KJ/mol and 173.50 J/mol respectively. The adsorption of crude palm oil became spontaneous at 363 and 373 K due to the negative values of Gibb's free energy obtained at those temperatures. The experimental result indicates that 83.2% bleaching efficiency can be from bleaching crude palm oil with alkaline-activated Amansea clay.



*Keywords: [Bleaching; crude palm oil; Amansea clay; alkaline activation; adsorption kinetics; equilibrium isotherms; thermodynamics study}*


## 1. INTRODUCTION

Palm oil is used for cooking food. They are also used in industries for producing margarine, shortening, cleaning soaps, detergents and manufacturing cosmetics [1]. However, crude palm oil has an orange-reddish colour because of its high content of carotenoids [1,2]. It also contains impurities like free fatty acid, fatty acid polymer, xanthophylls, carotenoid acids, chlorophyll, tocopherols and gossypol, solid triacylglyceride, pigments, phosphatides and parsia glycerides [3,4,2]. These pigments and impurities affect negatively the taste of palm oil thereby limiting its marketability and use [5]. Hence, the need to purify crude palm oil to remove the impurities and odour through an adsorptive bleaching process to make it acceptable for consumption and industrial purposes [1,4,2]. Types of bleaching methods include heat bleaching, chemical oxidation, and adsorption [1,5]. The advantage of adsorptive bleaching is that the pigment is removed from the oil without affecting the consistency of the oil [1]. In addition, the pro-oxidative properties that promote oxidation and reduce the oil quality are also removed during bleaching [5]. Many types of adsorbents including imported clays have been applied for the removal of pigments from palm oils [4]. However, the use of natural clay is more economical than imported clay [6].

Natural clay is highly abundant in Nigeria [4]. "Natural clay such as fuller's earth and bentonite have been applied as bleaching clay to remove colour impurities from crude palm oil. However, researchers have proved that the adsorptive properties of clay improved when activated before the bleaching process" [4]. There is need to investigate the modification of Nigerian clay for the industrial applications of palm oil refining. The activation of clay is the application of physical and chemical treatment on clay to improve its ability to remove unwanted properties [4]. Activation modifies the surface of the clay, increases its surface area by reducing its particle size, and changes its chemical composition through ionic

exchange and its texture. This improves the clay's capacity to adsorb color and other impurities in vegetable and animal oils [6]. Acid activation has been successfully and commonly applied on clays to be used as adsorbent in bleaching crude palm oil [4]. Increase in the concentration of acid and temperature has been reported to improve the bleaching capacity of clay [6]. "Generally, the factors that influence the bleaching performance of activated clay include the concentration of the activated clay, the bleaching temperature, the activation temperature, clay dosage, moisture content clay quality, particle size and bleaching time" [7].

Acid activation have been successfully and commonly applied but the removal of residual acid is a drawback because it causes environmental pollution by creating an acidic waste stream, reduces the quality of the bleached oil due to the effect of acid on the oil constituents, and consumes time and energy. It also causes soap formation during neutralization and the cost of production is increased as the bleached oil has to be neutralized with an alkaline solution [7,4]. "The cost of acid is also high thereby leading to the need for alkaline activation as an alternative method of improving the adsorptive properties in natural clay for crude palm oil bleaching" [7]. Some researchers have investigated the suitability of alkaline-activated clays in the bleaching of palm oil. These authors discovered that the alkaline clay showed a change in its morphological structure and increased the adsorptive capacity of the clay to up to 79% at the optimum concentration of 1.0 N NaOH [7]. [4] obtained a color reduction of 30.20 and 27.50% from NaOH and KOH activated clay respectively.

"Raw and activated clays contain many components of which some may be contaminants" [6,8]. Ionic metals such as Pb, Hg, Fe, Zn, Cu, Co, Cr, Mn, and Ni are required in minute amounts in biological systems for the purpose of metabolism, but at higher dosage can cause sicknesses such as cancer, cardiovascular and kidney diseases to the living [8]. The characteristics of clays change after acid or alkali activation and also on the concentration applied [9]. It is important to determine the metals present in the clays and how contaminants can be eliminated before the clay is used in bleaching edible oils. Clay composition includes elemental, mineralogical and biological constituents [9,6]. The knowledge of heavy and trace metals in clays from analyses reduces the risk of product contamination. The analysis of clay using X-ray fluorescence (XRF) is often more appropriate where the total elemental concentration of geological materials such as many rocks and soils is required [6]. The Fourier transform infrared spectroscopy (FTIR) can be used to observe the absorption bands of the chemical composition of both raw and activated clays [10]. Scanning electron microscopy (SEM) analysis helps to identify the clay's microstructure or its bonding structure [11]. From the performance of the experiment, a suitable clay is developed for the effective bleaching of crude palm oil with minimum contaminants[8].

"Thermodynamics and kinetics studies show the mechanism and degree of the overall performance of the adsorption process" [1]. "The adsorption isotherm determines the equilibrium relationship between the concentration in the fluid phase and adsorbent particles at a given temperature" [5]. An isotherm describes the relationship between the coverage of the surface of the adsorbent and the partial pressure of adsorbate gas at a constant temperature [6]. Hence, this study was aimed at characterizing the raw and alkaline-activated sample clay from Amansea, Nigeria, observing the bleaching performance of the activated clay, and evaluating the kinetic, equilibrium isotherm and thermodynamic studies of the bleaching process. The results obtained from this study will increase the available knowledge on alkaline activation and provide data for industrial large-scale production of alkaline activated clay thereby reducing importation which will help in boosting the Nigerian economy through the application of locally-sourced clay.

## 2. MATERIAL AND METHODS

The materials and methods applied in carrying out the bleaching experiment are shown in this section.

### 2.1 Materials

The clay sample used for the experiment was off-white and obtained from Amansea (6.2632□N, 7.1264□E) in Anambra State, Nigeria. The raw clay sample was grinded to pass through a 150 µm mesh sieve after drying at 105oC for 4 hr. The crude palm oil was obtained from a palm oil plant located in Ifite, Awka. The sodium hydroxide (NaOH) and potassium hydroxide (KOH) used in this process were of analytical grade.

### 2.2 Clay Characterization

The raw and activated clay samples produced were characterized using X-Ray Fluorescence spectroscopy (XRF), Fourier Transformed Infrared Spectroscopy (FTIR) and Scanning Electron Microscopy (SEM). The chemical composition of the raw and activated clay samples was determined using a model - X- supreme 8000 XRF equipment [7]. The functional groups in the raw and activated clays were recorded on a Shimadzu S8400 spectrophotometer in the range of 650-4000

$cm^{-1}$. The surface morphology of the clays was evaluated on a Phenom Proxy, PW 100-002 microscope, at a magnification of 225x [12,13].

## 2.3 Alkaline Activation of the Clay Sample

150 g of the sieved raw clay was mixed with 500 ml of a mixture of 5 M and 0.5 M of potassium hydroxide (KOH) and sodium hydroxide (NaOH) respectively. The slurry was heated at 100 oC for 2 hrs while being continuously stirred during the heating process. At the end of the alkaline activation, the slurry was cooled in the air at room temperature, filtered and the activated clay (AAMC) was washed with distilled water to a neutral pH (≈7). The activated clay (AAMC) was dried in a memmert oven at 105 oC for 24 hrs, ground and sieved using a150 µm mesh size.

## 2.4 Degumming

1000 ml of boiled water was poured into 500 ml of the crude palm oil contained inside a 2000 mL beaker. A separating funnel was used to separate the gum and water from the hot palm oil. This process was repeated until most of the hydratable gums were removed.

## 2.5 Bleaching Process

The bleaching process is always carried out under steam, vacuum or nitrogen in other to reduce the oxidation of oils by oxygen at elevated temperatures [6].

### 2.5.1Experimental procedure

A known quantity of the degummed crude palm oil (100 ml) was put into a beaker of 500 ml capacity and heated in a magnetic stirrer hot plate (model: SH85-2) to the required temperature. The alkaline-activated clay (1 g) was then added to the beaker, and fitted with a magnetic stirrer. The mixture was stirred continuously as it was heated at contact times of 10, 20, 30, 40, 45, and 50 mins. At the end of the bleaching process, the oil and clay mixture were filtered using a filter paper (Whatman No. 1) and the absorbance of the bleached oil was tested using an ultra violet-visible spectrophotometer (model no - 752, P/N: C001). The absorbance of the bleached oils was determined at 550 nm wavelength for each oil sample obtained after bleaching at different process temperatures. The experiments were carried out at temperatures of 50, 70, 90, and 100 oC. The bleaching experiment was carried out as a batch process.

The equilibrium adsorption experiment was carried out using different activated clay dosages (1.0, 1.5, 2.0, 2.5, 3.0, and 7.0 g by weight). The bleaching procedure was carried out at the operating temperature of 100 oC and contact times of 10, 20, 30, 40, 45, and 50 mins. This was done to investigate the percentage decrease in absorbance of bleached palm oil as the mass of clay increased [6].

### 2.5.2 The bleaching performance

The performance of the bleaching process and the percentage color reduction were evaluated from the decrease in absorbance [6]. The samples were diluted in acetone to a concentration of 10% (v/v) before the absorbance reading. It was calculated as given in equation (1).

$$Bleaching\ performance\ (\%) = \frac{A_o - A_t}{A_0} \times 100\% \qquad (1)$$

Where $A_o$ and $A_t$are the absorbances of crude oil and bleached oil at time, $t$ respectively.

## 2.6 Adsorption kinetics experiment

The adsorption kinetic studies give information on the efficiency of the adsorption process. It reveals the rate of the reaction of the solute uptake [14]. However, the kinetic models do not show the actual cause of adsorption [15]. The intra-particle diffusion model was simulated in the results obtained to evaluate the mechanism controlling the adsorption process [16,14]. The effect of contact time on the bleaching efficiency of crude palm oil using AAMC was tested with four kinetic models tabulated in Table 1.

**Table 1. Adsorption kinetic models fitted into the bleaching process using AAMC**

| Kinetic model | Kinetic equation | Reference |
|---|---|---|
| Pseudo-first-order | $\ln(q_e - q_t) = \ln q_e - K_1 t$ (2) | [17] |
| Pseudo-second-order | $\frac{t}{q_t} = \frac{1}{K_2 q_e^2} + t(\frac{1}{q_e})$(3) | [12] |
| Intra-particle | $q_t = K_d t^{0.5} + \varepsilon$ (4) | [17] |
| Elovich | $q_t = \frac{1}{\beta}\ln(\alpha\beta) + \frac{1}{\beta}\ln t$(5) | [16] |

## 2.7 Equilibrium isotherm modelling

Equilibrium adsorption isotherm study is an important factor that optimizes the application of adsorbents by describing the interactions between the adsorbate and the adsorbent. The isotherm studies are carried out through the ratio of the absorbed quantity to the concentration of adsorption equilibrium or pressure at a constant temperature [18]. The isotherm studies evaluate the relationship between the amount and concentration of a substance removed from a liquid phase per unit mass of adsorbent at a constant temperature. Its application is useful in the design of adsorption systems [14]. The experimental data were simulated into the linear form of the Langmuir, Freundlich, Temkin and Dubinin–Radushkevich isotherm models as shown in Table 2.

**Table 2. Equilibrium isotherm models fitted into the bleaching process using AAMC**

| Isotherm model | Isotherm equation | Reference |
|---|---|---|
| Langmuir | $\frac{X_e}{q_e} = \frac{1}{K_1 q_m} - \frac{X_e}{q_m}$ (6) | [17] |
| Freundlich | $log\ q_e = \log K + \frac{1}{n} log\ X_e$ (7) | [16] |
| Temkin | $q_e = B_1 lnK_T + B_1 lnX_e$ (8) | [17] |
| Dubinin-Radushkevich | $lnq_e = \ln Q_m - \beta\varepsilon^2$ (9) | [19] |
| (D-R) | $\varepsilon = RTln(1 + \frac{1}{C_e})$ (10) | [19] |

## 2.8 Adsorption thermodynamics

The study and determination of the thermodynamic properties are necessary to determine the feasibility and spontaneity of the process [1,15]. The thermodynamic parameters are evaluated easily because the adsorptive bleaching process is a temperature dependent process. These thermodynamic parameters include the Gibbs free energy ($\Delta G^o$), change in enthalpy ($\Delta H^o$), and change in entropy ($\Delta S^o$). These parameters were calculated using Equations (11), (12), (13) and (14). The Gibbs free energy of change evaluates the spontaneity of the process [15].

$$\Delta G^o = -RTln(k_d) \quad (11)$$

where

$\Delta G^o$ (J/mol) is Gibb's free energy change, R is the universal gas constant (8.314 $Jmol^{-1}K^{-1}$), T is the absolute temperature (K) and $k_d$ is the thermodynamic equilibrium constant or distribution coefficient. This equation measures the changes in the equilibrium constant with temperature variations [15].

The enthalpy change ($\Delta H^o$) is the energy supplied in the form of heat at constant pressure when no extra work is done by the system. The change in enthalpy gives information on the nature and mechanism of the adsorption process. The change in entropy ($\Delta S^o$) shows the randomness at the solid/liquid interface with some changes in the structure of the adsorbent and adsorbate [15]. The change in enthalpy and entropy are obtained from the Van't Hoff equation [15,20].

$$\ln k_d = \frac{\Delta S}{R} - \frac{\Delta H}{RT} \quad (12)$$

Where the value of $k_d$ is calculated from equation (16) [21];

$$k_d = \frac{q_e}{X_e} \quad (13)$$

and

$$\Delta G = \Delta H - T\Delta S \quad (14)$$

The values (in J/mol) of the enthalpy ($\Delta H^o$) and entropy ($\Delta S^o$) are estimated from equation (12) whereas the values of $\Delta G^o$ are calculated from Equation (14) [1,21]. The values of $\Delta H^o$ and $\Delta S^o$ were evaluated from the slope and intercept of the linear plot of ln $k_d$ against 1/T using Equation (12).

## 3. RESULTS AND DISCUSSION

### 3.1 Characterization of the Adsorbent

The results of the FTIR, SEM and XRF analyses are shown below.

#### 3.1.1 Fourier transform infrared spectroscopy (FTIR) analysis

The importance of the study of the chemical structure of adsorbents lies in the ability to understand the adsorption process. The FTIR analysis of the clay sample used for bleaching crude palm oil helps to identify the minerals present in the clay and also the characteristic functional groups present during the adsorption of aromatic compounds [5]. The FTIR results of the raw and alkaline-activated Amansea clay samples were assigned according to the functional groups reported by [22,23,24,25,26]. The infrared spectra were obtained for the samples before and after the activation process with 5 M and 0.5 M of potassium hydroxide (KOH) and sodium hydroxide (NaOH) respectively at 100 oC for 2 hours in a wavenumber range of 4000 – 650 $cm^{-1}$. The functional groups and their frequencies are shown in Table 2. It was observed that there were modifications on the clay sample after alkaline activation when compared to the raw clay as seen in Figs. 1 and 2 and in Table 3 [5]. The maximum adsorption band was reduced after the activation of Amansea clay sample. The wavenumbers between 3700 – 3600 $cm^{-1}$ for raw and activated Amansea clay samples correspond to Al–O–H stretching [5,13]. The bond source (Al–O–H stretching) present confirms the presence of the Kaolinite mineral in the clay samples. The strong bands in the region of 1120-1000 $cm^{-1}$ in both untreated and treated clays are assigned to Si-O stretching vibration of kaolinite clay [10,13]. In addition, an old peak disappeared at 682.1 $cm^{-1}$ in the raw clay after acid-activation. Isothiocyanate (–NCS) bond was found at 2079.9 and 2050 $cm^{-1}$ while Vinyl C–H out of plane bend was observed at 909.5 and 913.2 $cm^{-1}$ [22,24,26]. Hence, the Amansea clay is dominantly Kaolinite [5].

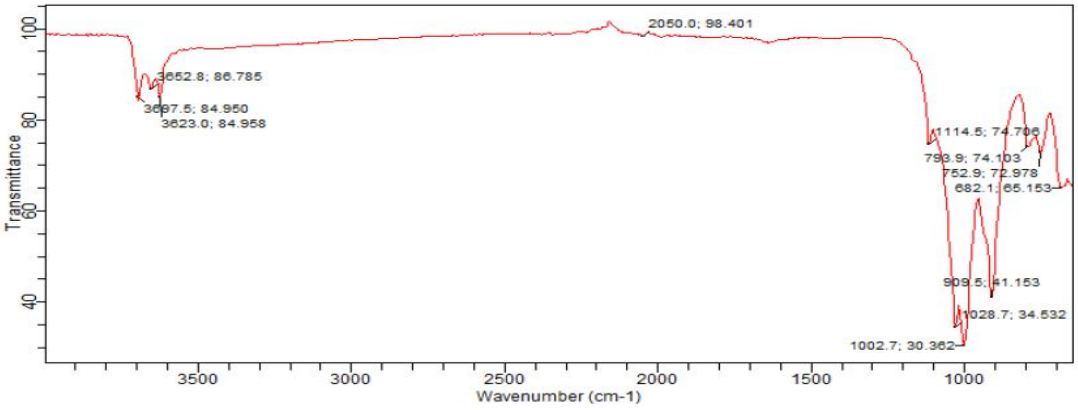


**Fig. 1. FTIR result of raw Amansea clay**

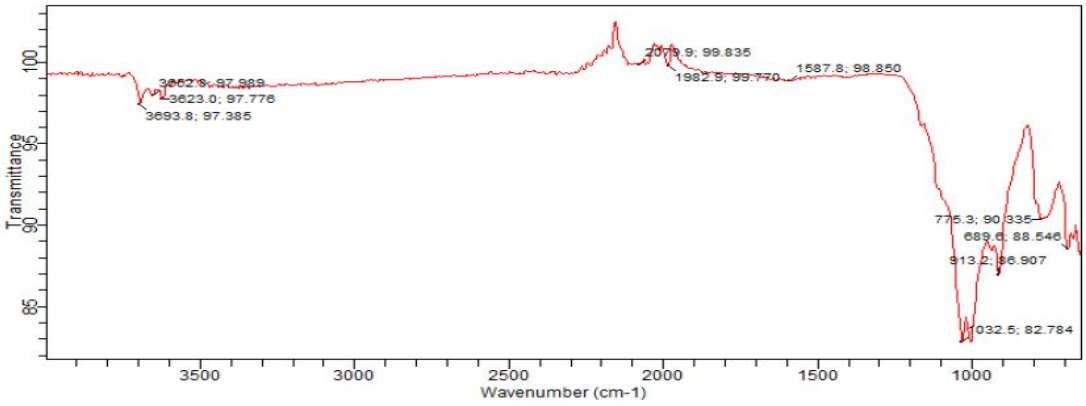


**Fig. 2. FTIR result of alkaline-activated Amansea clay (AAMC)**

**Table 3. Comparison of FTIR spectra of raw and alkaline-activated Amansea clay**

| Raw or un-activated clay ($cm^{-1}$) | Acid activated clay ($cm^{-1}$) | Range of assignment ($cm^{-1}$) | Assigned organic structure | Reference |
|---|---|---|---|---|
| 3697.5 | 3693.8 | 3700 - 3600 | Al–O–H stretching | [5,13] |
| 3652.8 | 3652.8 | 3700 - 3600 | Al–O–H stretching | [5,13] |
| 3623.0 | 3623.0 | 3700 - 3600 | Al–O–H stretching | [24,13] |
| 2050.0 | 2079.9 | 2200 - 2000 | Isothiocyanate (–NCS) | [22,26] |
| 1114.5 | 1982.9 | 1225 - 950 | Si–O stretching vibration | [10,5] |
| 1028.7 | 1587.8 | 1225 - 950 | Si–O stretching vibration | [10,5,13] |
| 1002.7 | 1032.5 | 1225 - 950 | Si–O stretching vibration | [5,13] |
| 909.5 | 913.2 | 915 - 890 | Vinyl C–H out-of-plane bend | [24,26] |
| 793.9 | 775.3 | 900 – 670 | Aromatic C–H out-of-plane bend | [24,26] |
| 752.9 | 689.6 | 900 – 670 | Aromatic C–H out-of-plane bend | [24,26] |
| 682.1 | - | 900 – 670 | Aromatic C–H out-of-plane bend | [24,26] |

### 3.1.2 Scanning electron microscopy (SEM) analysis

The SEM micrograph view features such as cracks, veins and fissures [27]. Clay minerals can be identified and characterized by their morphological features. Figs. 3 and 4 show the results of SEM analysis of the raw and alkaline-activated Amansea clay samples respectively. SEM analysis shows the morphology, surface structure and crystalline structure of both adsorbents. The SEM analysis in Figs. 3 and 4 indicated that the adsorbents were loosely packed, and very coarse with hexagonal irregular edges confirming that the clays were Kaolinites [5]. The raw clay revealed the presence of large particles which were formed by several flakes of particles that became stacked together forming agglomerates. The SEM images of alkaline-activated clay (AAMC) showed the reduction in size and the disaggregation of clay structure due to the action of heat and alkaline treatment [27,13]. The treated clay sample was no longer as intact as the raw clay because some minerals were removed from it leading to an increase in the microporous surface. These observations revealed that the alkaline-activation was properly done [27].

**Fig. 3. SEM analysis of Amansea clay before activation (100 µm)**

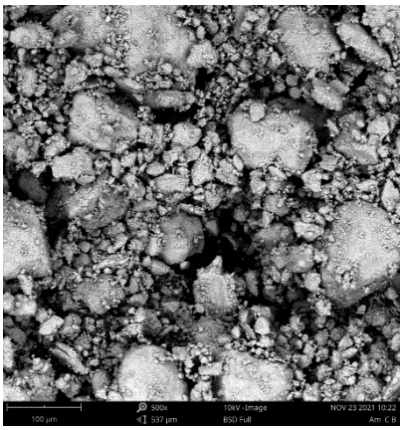

**Fig. 4. SEM analysis of Amansea clay (AAMC) after activation (100**

### 3.1.3 X-ray Fluorescence (XRF) analysis

The chemical composition of the minerals in the raw and activated clay samples were determined using X-ray Flourescence (XRF) [22,5]. The XRF analysis is also applied in the stabilization of the elemental composition of solid materials [28]. Tables 5 and 6 showed the results of the oxides and elements present in both raw and alkaline-activated Amansea clay samples.

The major oxides present in the raw and alkaline-activated clay samples were $SiO_2$, $Al_2O_3$, $K_2O$, CaO, TiO2, MnO and $Fe_2O_3$ [21,7]. The silica oxide content in the raw clay was seen to increase from 55.9% and 73.9% after alkaline-activation. The high content of silica oxide indicated that they can be used as a source of silica for the production of floor tiles [29]. Traces of other elements and oxides including copper, zinc, nickel and calcium, were also observed to be present in both clay samples. The chemical composition obtained in this work was also similar to [22,29]. The presence of impurities like Cl, $TiO_2$, ZnO, and $Cr_2O_3$ were observed during the analysis due to the inherent binding compounds in the clay samples [28]. The presence of $TiO_2$ in the clay samples was due to the presence of impurities such as rutile [7]. These were seen to reduce in the activated clay. The alkaline fluxes content in the form of $K_2O$ increased from 0.251 to 3.061% after activation. The presence of MgO and CaO showed that the clay samples are non-carbons [30]. Part of $Fe^{2+}$ was removed when alkaline activation was carried out. Phosphorus oxide was seen in trace quantity in the raw clay but disappeared after activation. This substitution led to the production of more negative charges on the clay surface which led to improved adsorption efficiency during the bleaching process. More active sites were produced on the activated clay surface from the XRF result because the fact that some interlayer cations were removed during activation [7].

228

229 **Table 4. The XRF result of oxides from raw and activated Amansea clay samples**

| Oxide | Concentration in % (raw clay) | Concentration in % (alkaline-activated AAMC) |
|---|---|---|
| $SiO_2$ | 55.869 | 73.896 |
| $V_2O_5$ | 0.127 | 0.065 |
| $Cr_2O_3$ | 0.046 | 0.113 |
| MnO | 0.085 | 0.032 |
| $Fe_2O_3$ | 12.100 | 4.285 |
| $CO_3O_4$ | 0.052 | 0.017 |
| NiO | 0.001 | 0.002 |
| CuO | 0.039 | 0.052 |
| $Nb_2O_3$ | 0.018 | 0.008 |
| $MoO_3$ | 0.003 | 0.001 |
| $WO_3$ | 0.000 | 0.004 |
| $P_2O_5$ | 0.038 | 0.000 |
| $SO_3$ | 0.795 | 0.120 |
| CaO | 0.219 | 0.235 |
| MgO | 0.000 | 0.000 |
| $K_2O$ | 0.251 | 3.061 |
| BaO | 0.000 | 0.069 |
| $Al_2O_3$ | 26.285 | 15.373 |
| $Ta_2O_5$ | 0.022 | 0.043 |
| $TiO_2$ | 2.656 | 1.519 |
| ZnO | 0.007 | 0.002 |
| $Ag_2O$ | 0.020 | 0.007 |
| Cl | 0.612 | 0.990 |
| $ZrO_2$ | 0.311 | 0.076 |
| $SnO_2$ | 0.000 | 0.000 |
| PbO | 0.407 | 0.022 |
| $Rb_2O$ | 0.004 | 0.001 |
| SrO | 0.032 | 0.005 |

230

231 **Table 5. XRF result of the element from raw and activated Amansea clay samples**

| Element | Concentration in % (raw clay) | Concentration in % (alkaline-activated AAMC) |
|---|---|---|
| O | 47.669 | 49.274 |
| Mg | 0.000 | 0.000 |
| Al | 13.912 | 8.136 |
| Si | 26.116 | 34.542 |
| P | 0.017 | 0.000 |
| S | 0.319 | 0.048 |
| Cl | 0.612 | 0.990 |
| K | 0.208 | 2.541 |
| Ca | 0.156 | 0.168 |
| Ti | 1.593 | 0.910 |
| V | 0.071 | 0.037 |
| Cr | 0.032 | 0.078 |
| Mn | 0.066 | 0.025 |
| Fe | 8.463 | 2.997 |
| CO | 0.038 | 0.012 |
| Ni | 0.001 | 0.002 |
| Cu | 0.031 | 0.041 |
| Zn | 0.006 | 0.002 |
| Rb | 0.004 | 0.001 |
| Sr | 0.027 | 0.004 |
| Zr | 0.230 | 0.056 |

| | | |
|---|---|---|
| Nb | 0.015 | 0.007 |
| MO | 0.002 | 0.001 |
| Ag | 0.019 | 0.006 |
| Sn | 0.000 | 0.000 |
| Ba | 0.000 | 0.062 |
| Ta | 0.018 | 0.035 |
| W | 0.000 | 0.003 |
| Pb | 0.378 | 0.021 |

## 3.2 Effect of Process Parameters on the bleaching efficiency

The absorbance value of the crude palm oil sample was 2.50. The effects of contact time, temperature and adsorbent dosage on the bleaching efficiency were also evaluated.

### 3.2.1 Effect of contact time on the bleaching efficiency

The effect of the contact time on the bleaching efficiency was investigated from the absorbance measurement at different temperatures. There was a percentage decrease in the absorbance of the bleached oil as the contact time increased. This led to a percentage increase in bleaching efficiency as contact times were increased. Adsorption processes involve the migration of the adsorbate to the boundary layer after which there is the diffusion of the adsorbate onto the adsorbent surface before diffusing into the porous adsorbent structure [31]. The data on absorbance and efficiencies of crude palm oil bleaching are shown in Tables 6 and 7. The plot of the effect of contact time on bleaching efficiency is shown in Fig. 5. Reduction in both absorbance and improved bleaching efficiencies on oil bleaching has also been observed with activated clays [1,32,31,5]. Little significance was observed in the change in the percentage of the absorbance and bleaching efficiency when the sample was heated for more than 45 minutes. There was a less significant increase in adsorption capacity after 45 minutes because there were lesser active sites in the clay dosage. Afterall, the clay sites became saturated at that contact time [31]. [1] observed no significant change in the absorbance reading after 40 minutes. Researchers have stated that the contact time for effective bleaching ranged from 15 to 45 minutes and that activated clay had more adsorptive sites, pore size and surface area than raw clay. The highest bleaching efficiency obtained during the experiment was 76.8%. This showed that the alkaline-activated Amansea clay is a good adsorbent for the bleaching of crude palm oil. The value of the percentage bleaching efficiency obtained was a result of the alkalinity used for clay activation and the high crystallinity of the kaolin clay [1].

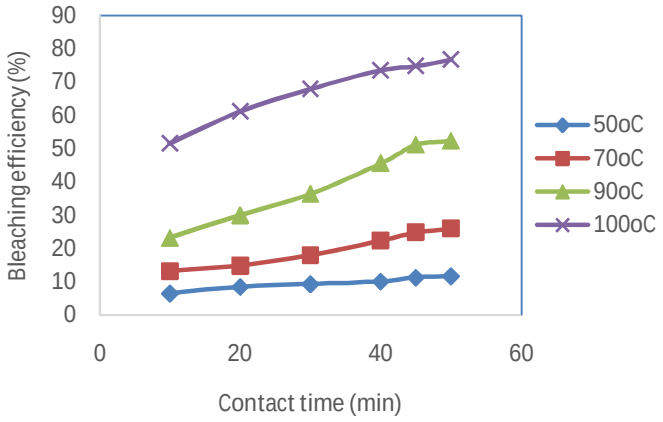


**Fig. 5. Effect of Contact time on bleaching performance**

### 3.2.2 Effect of temperature on the bleaching efficiency

The plot of the effect of temperature on the bleaching efficiency is shown in Fig. 6. It was observed that the percentage of bleaching efficiency increased with an increase in temperature [1,5,29]. The highest bleaching efficiency was obtained at 100 oC temperature as also reported by [29]. Activated local clays have been observed to only improve the bleaching efficiencies at higher temperatures when compared to imported bleaching earth [5]. Increasing the temperature improves

the dispersion of particles thereby increasing the palm oil-clay interactions and ability to flow. The increase in available sites led to an increase in pigment removal thereby improving the bleaching efficiency. The optimum bleaching temperature for palm oil bleaching is usually between 100-120 oC. The bleaching efficiency increased at high temperatures due to a reduction in viscosity which increases the speed of molecules/diffusion rate of the adsorbent particles leading to better interaction between the adsorbent and the oil [1,31]. High temperatures also lead to an increase in the capacity of equilibrium of the adsorbent [31].

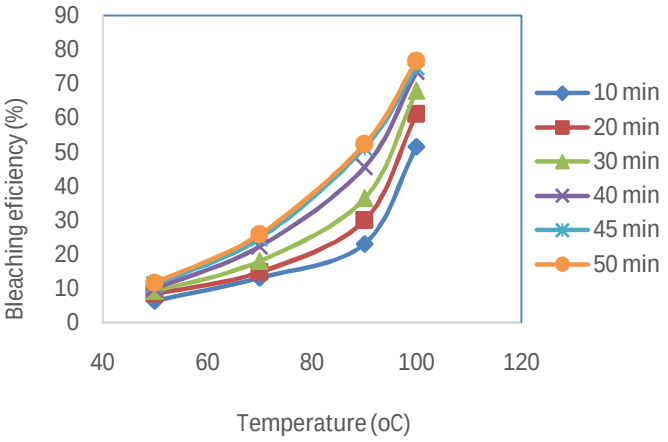


**Fig. 6. Effect of temperature on bleaching performance**

**Table 6. Experimental data for palm oil bleaching using 1 g AAMC at different temperatures and contact time**

| Time (min) | Absorbance reading | | | |
|---|---|---|---|---|
| | 50 oC | 70 oC | 90 oC | 100 oC |
| 10 | 2.34 | 2.17 | 1.92 | 1.21 |
| 20 | 2.29 | 2.13 | 1.75 | 0.97 |
| 30 | 2.27 | 2.05 | 1.59 | 0.80 |
| 40 | 2.25 | 1.94 | 1.36 | 0.66 |
| 45 | 2.22 | 1.88 | 1.22 | 0.63 |
| 50 | 2.21 | 1.85 | 1.19 | 0.58 |

**Table 7. Bleaching efficiencies of 1 g AAMC on crude palm oil at different temperatures and contact time**

| Time (min) | Bleaching performance (%) | | | |
|---|---|---|---|---|
| | 50 oC | 70 oC | 90 oC | 100 oC |
| 10 | 6.4 | 13.2 | 23.2 | 51.6 |
| 20 | 8.4 | 14.8 | 30 | 61.2 |
| 30 | 9.2 | 18 | 36.4 | 68.0 |
| 40 | 10 | 22.4 | 45.6 | 73.6 |
| 45 | 11.2 | 24.8 | 51.2 | 74.8 |
| 50 | 11.6 | 26 | 52.4 | 76.8 |

### 3.2.3 Effect of adsorbent dosage on the bleaching efficiency

It could be observed from Fig. 7 that the bleaching efficiency also increased with an increase in the adsorbent dosage [1,5]. The data on absorbance and bleaching efficiency of the bleached crude palm oil at a constant temperature of 100 oC is given in Tables 8 and 9 respectively. The absorbance of unbleached crude palm oil was 2.5 at 550 nm before the oil underwent the treatment to improve its color. The activated clay has been known to have more adsorptive sites, and increased pore size and surface area than other clays, thereby increasing its adsorption efficiency [27,31]. The adsorption sites increased as the adsorbent dosage increased [31]. When the oil was treated with AAMC, the absorbance of the bleached oils decreased with an increase in contact time. No significant percentage change in absorbance was observed

when the sample was heated for more than 40 minutes. Researchers have reported that the contact time for effective bleaching ranges from 15 to 45 minutes [1]. The highest bleaching efficiency observed was 83.2% at 50 minutes using 3 g of AAMC. It was observed that increasing the dosage of activated clay to 7 g using the same quantity of crude palm oil reduced the equilibrium concentration in the medium thereby reducing the adsorption capacity [18]. [6] observed a decrease in the absorbance of the bleached oils following the increase in the adsorbent dosage of acid-activated Kangole clay by up to 4%. However, they reported that there was no significant decrease in the oil absorbance beyond 4% as adsorption equilibrium had been attained between the activated clay and oil mixtures, which prevented further color removal by the increased adsorbent dosage.

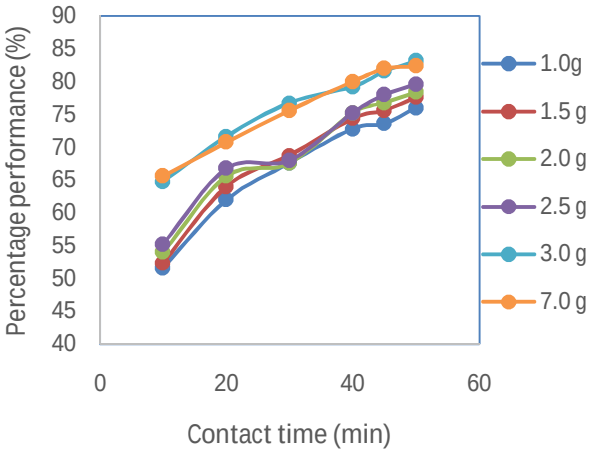


**Fig. 7. Effect of clay dosage on bleaching performance**

**Table 8. Absorbance results from varying dosage and contact time of AAMC at 100 oC**

| Time (min) | Absorbance | | | | | |
|---|---|---|---|---|---|---|
| | 1 g | 1.5 g | 2.0 g | 2.5 g | 3 g | 7g |
| 10 | 1.21 | 1.19 | 1.15 | 1.12 | 0.88 | 0.86 |
| 20 | 0.95 | 0.90 | 0.86 | 0.83 | 0.71 | 0.73 |
| 30 | 0.81 | 0.78 | 0.81 | 0.80 | 0.58 | 0.61 |
| 40 | 0.68 | 0.64 | 0.62 | 0.62 | 0.52 | 0.50 |
| 45 | 0.66 | 0.61 | 0.58 | 0.55 | 0.46 | 0.45 |
| 50 | 0.60 | 0.56 | 0.54 | 0.51 | 0.42 | 0.44 |

**Table 9. Bleaching efficiencies from varying dosage and contact time of AAMC at 100 oC**

| Time (min) | Bleaching efficiency (%) | | | | | |
|---|---|---|---|---|---|---|
| | 1 g | 1.5 g | 2.0 g | 2.5 g | 3 g | 7g |
| 10 | 51.6 | 52.4 | 54.0 | 55.2 | 64.8 | 65.6 |
| 20 | 62.0 | 64.0 | 65.6 | 66.8 | 71.6 | 70.8 |
| 30 | 67.6 | 68.8 | 67.6 | 68.0 | 76.8 | 75.6 |
| 40 | 72.8 | 74.4 | 75.2 | 75.2 | 79.2 | 80.0 |
| 45 | 73.6 | 75.6 | 76.8 | 78.0 | 81.6 | 82.0 |
| 50 | 76.0 | 77.6 | 78.4 | 79.6 | 83.2 | 82.4 |

## 3.3 Adsorption Kinetics

The kinetic studies on the adsorptive bleaching of crude palm oil using AAMC was carried out to reveal the rate of the uptake of the adsorbate and to observe the mechanism of adsorption and the rate controlling steps which are important in the decision to carry out the full-scale batch processes [1,31]. Adsorption kinetic models have been classified into adsorption reaction models and adsorption diffusion models [15]. Pseudo-first order, pseudo-second order and Elovich

models are some of the adsorption reaction models which showed the rate of adsorbate uptake by adsorbents but do not reveal the cause of adsorption. However, the intraparticle diffusion model is one of the adsorption diffusion models which recognizes the internal or pore diffusion, external diffusion, and effect of mass action [15].

The experimental data obtained were tested with four kinetic models and the plots of the kinetic models are shown in Figs. 8-11. The kinetic constants which were obtained from the slopes and intercepts of the plots are shown in Table 10. The experimental adsorption capacities at equilibrium, *qe* were obtained as 0.12, 0.26, 0.52, and 0.77 at 50, 70, 90 and 100 oC respectively by plotting the adsorption capacities at different times, *qt* against time (in minutes) as shown in Fig. 12. [1] obtained the value of 0.26 as *qe* from the bleaching of palm oil with acid-activated kaolin clay at 120 oC. This value of *qe* obtained is comparable to the ones obtained for this work at the four temperatures applied. The difference in values when compared to [1] may have been due to the type of clay, the type of activation done on the clay and the concentration of the acid or alkaline applied to the clay. As seen from the results, the pseudo-second order kinetic model best fitted the experimental data since the $R^2$ values at all four temperatures showed very high fitness when compared to the other models, with the highest $R^2$ value obtained at 50 oC as 0.9975. [23,31,20] also observed that the pseudo-second order model best described the bleaching process. The Elovich and intra-particle models also provided a good fit as the average $R^2$ value obtained was >0.9. The experimental data obtained did not fit the pseudo first-order model due to its average $R^2$ value of <0.9, showing that the process was not a first-order reaction [31,33].

In the pseudo-second order model, the values of calculated qe were close to the experimental qe when compared to the other models, indicating that it better described the process than the other models. The equilibrium rate constant of the pseudo-second order model, $K_2$ (g/mg min) obtained at 50, 70, 90 and 100 oC were 0.0699, 0.0389, 0.0311 and 0.1233 respectively. The Pseudo-second order model gave high regression coefficients which was an indication that chemisorption was the rate-controlling step in the adsorption process [18,31]. Chemical adsorption or chemisorption is the process where there are chemical forces of attraction due to the pressure of the appeal current between the adsorbent and adsorbate during the formation of a layer of adsorbate on the adsorbent [1]. If the linear plot of qt versus $t^{1/2}$ passed through the origin, the intra-particle diffusion will be the sole rate-limiting process. However, the graph of the intra-particle model did not cut the origin indicating that diffusion was not the limiting step [18,14].

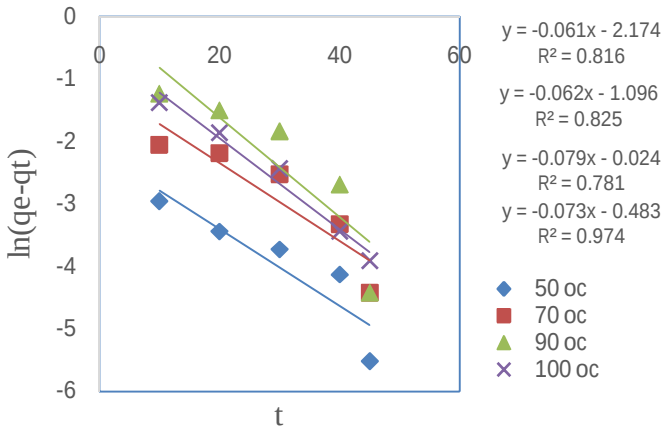


**Fig. 8. Plot of Pseudo first-order kinetic model**

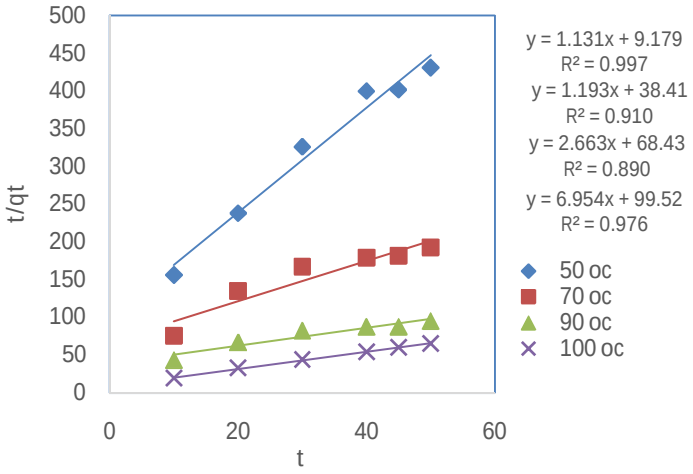


336

337 **Fig. 9. Plot of Pseudo second-order kinetic model**

338

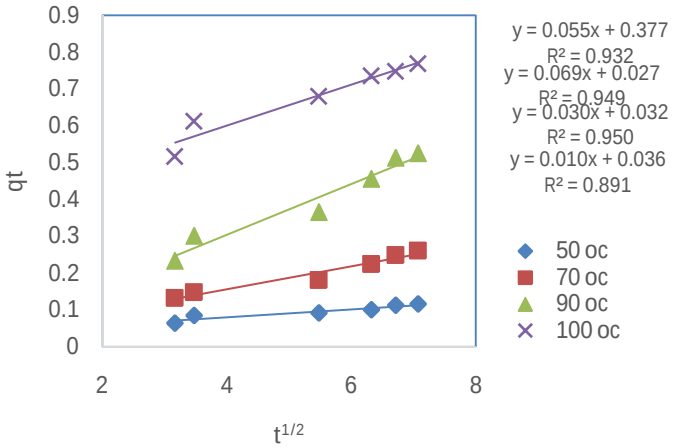


339

340 **Fig. 10. Plot of Intra-particle diffusion kinetic model**

341

342

343

344

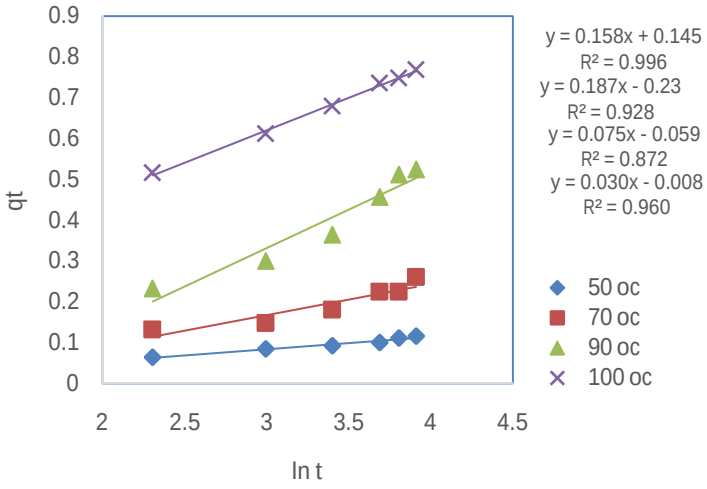


345

346 **Fig. 11. Plot of Elovich model**

347

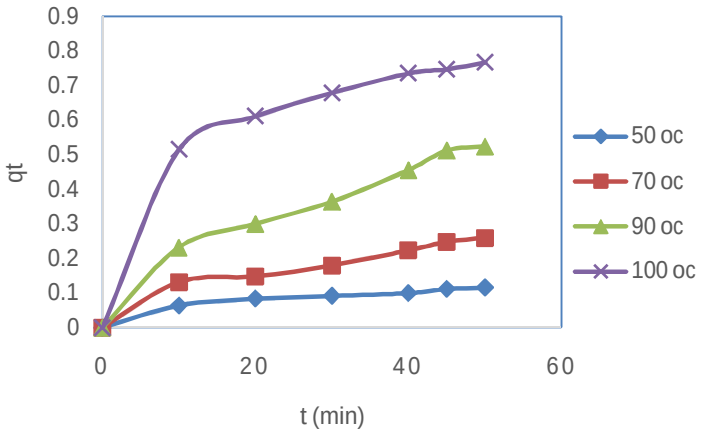


348

349 **Fig. 12. Plot of determination of qe**

350

351 **Table 10. Adsorption kinetic parameters for the bleaching of palm oil using AAMC**

| Kinetic model | Kinetic constants | Temperature (oC) | | | |
|---|---|---|---|---|---|
| | | 50 | 70 | 90 | 100 |
| Pseudo first-order | $K_1$ ($min^{-1}$) | 0.0731 | 0.0381 | 0.0623 | 0.0615 |
| | $q_e$ (mg/g) | 0.6169 | 0.3981 | 0.3340 | 0.1137 |
| | $R^2$ | 0.9743 | 0.8439 | 0.8255 | 0.8161 |
| Pseudo second-order | $K_2$ (g/mg min) | 0.0699 | 0.0389 | 0.0311 | 0.1233 |
| | $q_e$ (mg/g) | 0.1438 | 0.3755 | 0.8379 | 0.8835 |
| | $R^2$ | 0.9769 | 0.8905 | 0.9104 | 0.9978 |
| Intra-particle diffusion | $K_d$ | 0.0096 | 0.0565 | 0.0564 | 0.0963 |
| | $\varepsilon$ | 0.0366 | 0.0325 | 0.0278 | 0.3773 |
| | $R^2$ | 0.8918 | 0.9502 | 0.9491 | 0.9324 |
| Elovich | α | 0.0233 | 0.0346 | 0.0854 | 0.3977 |
| | β | 32.4675 | 13.1752 | 5.3362 | 6.3131 |
| | $R^2$ | 0.9602 | 0.8721 | 0.928 | 0.9966 |

352

### 3.4 Adsorption Isotherms

The adsorption isotherm studies were carried out using four isotherm models (Langmuir, Freundlich, Temkin and Dubinin-Radushkevich). The calculated isotherm constants from the four models are shown in Table 11. The values of $R^2$ from the isotherms were very high (>0.9) as also observed in [16]. However, the Temkin isotherm model gave the best fitting for the adsorption data because it displayed the highest $R^2$ values (>0.99) at all operating temperatures [21,34]. The plot of Temkin model at all temperatures are shown Figs. 13-16. The maximum adsorptive capacity ($q_m$) was also observed to increase as the operating temperature increased indicating that the adsorption process was an endothermic one [31]. The value of $q_m$ obtained in this work is comparable to the value reported by [22,31,6] where low values of $q_m$ (≤2) were also obtained after evaluation. Onu and Nwabanne [35] reported an adsorption capacity of 12mg/g using Nteje clay in adsorption.

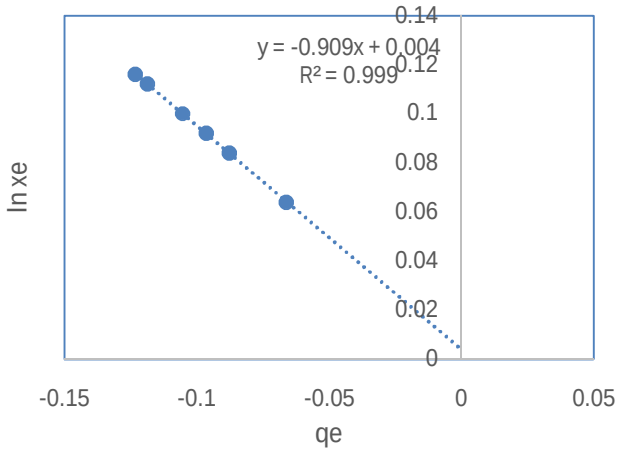


**Fig. 13. Plot of Temkin model at 50 oC**

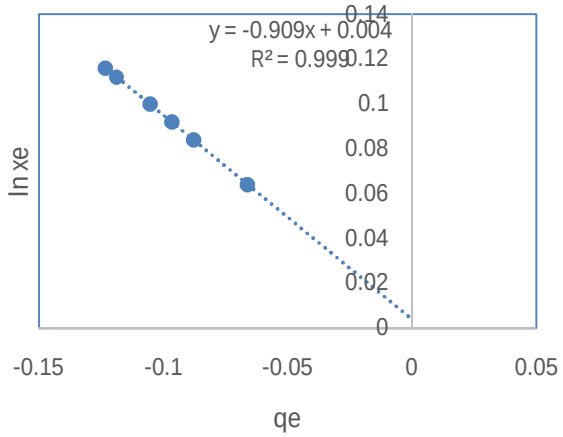


**Fig. 14. Plot of Temkin model at 70 oC**

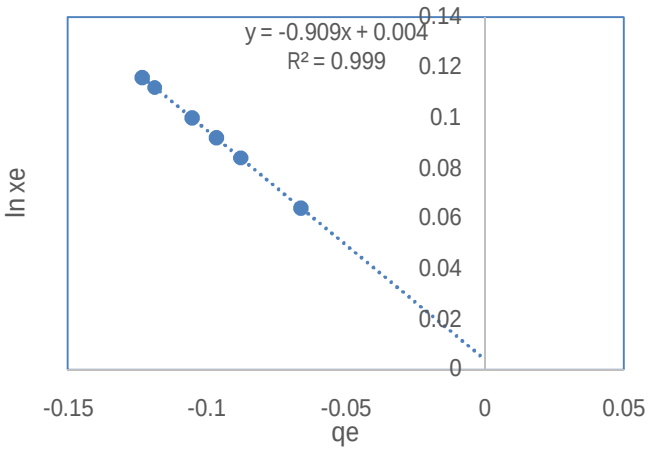


**Fig. 15. Plot of Temkin model at 90 oC**

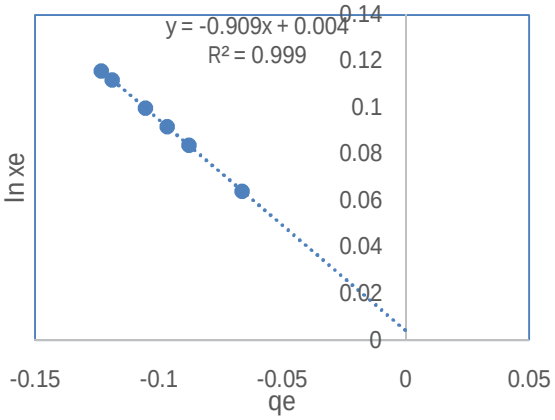


**Fig. 16. Plot of Temkin model at 100 oC**

**Table 11. Equilibrium isotherm parameters for the bleaching of palm oil using AAMC**

| Adsorption isotherm model | Kinetic constants | Temperature (oC) 50 | 70 | 90 | 100 |
|---|---|---|---|---|---|
| Langmuir | $K_1$ (l/mg) | - 0.8295 | - 0.6474 | - 0.3767 | - 0.1204 |
| | $q_m$ (mg/g) | 0.0091 | 0.0544 | 0.3434 | 3.3278 |
| | $R^2$ | 0.9655 | 0.974 | 0.9518 | 0.9883 |
| Freundlich | $K$ (l/g) | $5.15\times10^{-11}$ | $6.28\times10^{-5}$ | 0.0235 | 0.2942 |
| | $n$ | -0.6770 | -0.8902 | -1.2684 | -2.2614 |
| | $R^2$ | 0.9894 | 0.9902 | 0.9719 | 0.9769 |
| Temkin | $K_T$ (mg/g) | 0.9955 | 0.9759 | 0.8730 | 0.4376 |
| | $b$ (KJ/mol) | -2.953 | -3.556 | -5.000 | -9.121 |
| | $R^2$ | 0.9999 | 0.9996 | 0.9963 | 0.9903 |
| Dubinin-Radushkevich (D-R) | β | $-2.0\times10^{-68}$ | $-6.0\times10^{-7}$ | $-1.0\times10^{-7}$ | $-3.0\times10^{-8}$ |
| | $Q_m$ (mg/g) | $6.14\times10^{-5}$ | 0.0089 | 0.1043 | 0.3950 |
| | $R^2$ | 0.9871 | 0.9856 | 0.9491 | 0.9484 |

### 3.5 Thermodynamics studies

The values of enthalpy, $\Delta H^o$ and entropy, $\Delta S^o$were obtained from the slope and intercept of the plot of ln $k_d$ against 1/T in Fig. 12, where the $slope = \frac{-\Delta H^o}{R}$ and $intercept = \frac{\Delta S^o}{R}$ . The values of $\Delta H^o$ and entropy, $\Delta S^o$ and $\Delta G^O$ are shown in Table 12. The enthalpy change gives information about the nature and mechanism of an adsorption process. The positive value of $\Delta H^o$(61.9 KJ·mol$^{-1}$) calculated in this work indicates that the bleaching process of crude palm oil with AAMC was an endothermic one [15]. A similar result was reported for the basic dye on mansonia wood where the value of $\Delta H^o$ was 67.1 KJ·mol$^{-1}$. [33] reported a negative value of $\Delta H^o$ and concluded that the adsorption process was exothermic. The value of $\Delta H^o$ was also more than 40 KJ.mol$^{-1}$ implying that it was a chemisorption process [33]. The positive value of $\Delta S^o$ indicated that there was an increase in the randomness or degree of freedom at the solid/liquid interface of the activated carbon during the adsorption of beta carotene onto the active sites of AAMC [20]. It also showed that there was a high affinity of the adsorbent (AAMC) towards beta carotene [15].

Gibbs free energy evaluates the feasibility and spontaneity of an adsorption process. A negative ΔG$^o$ value validates a spontaneous process whereas a positive value of ΔG$^o$ indicates that the process is non-spontaneous [15,20,36,37]. The value of the Gibbs free energy change indicated that the bleaching of crude palm oil with AAMC was non-spontaneous at 323 and 343 K but became spontaneous as the bleaching temperature increased. This observation was also seen in [22]. Negative ΔG indicates spontaneous process [38]. The value of ΔG$^o$ decreased with an increase in temperature showing that the bleaching process was more favorable at higher temperatures [1].

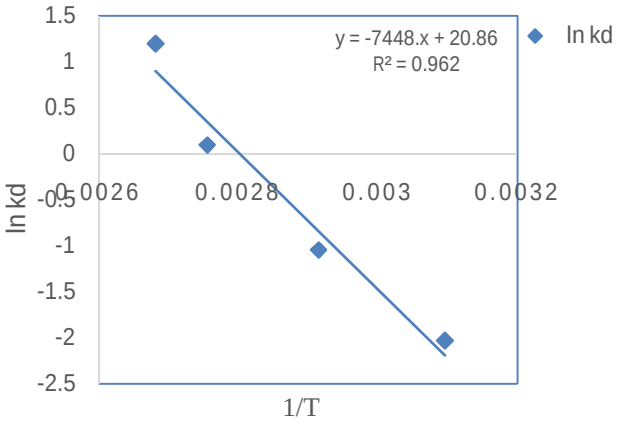


**Fig. 17. Thermodynamic plot of crude palm oil bleaching with AAMC at 100 oC**

**Table 12. Thermodynamic parameters from the bleaching of crude palm oil with AAMC**

| Temperature (K) | Thermodynamic properties | | |
|---|---|---|---|
| | $\Delta G^O$ (J/mol) | $\Delta H^o$ (J/mol) | $\Delta S^o$ (J/mol) |
| 323 | 5,884.67 | | |
| 343 | 2,414.67 | | |
| 363 | -1,055.33 | | |
| 373 | -2,790.33 | 61,925.17 | 173.50 |

## 4. CONCLUSION

Local clay from Amansea was used as a low-cost adsorbent in the bleaching of crude palm oil. The FTIR, SEM and XRF results after alkaline activation showed the characteristic functional groups, the morphological properties, the minerals,

and the numerous elements and compounds present in the clay. The analyses also revealed that the clay was kaolinite. An increase in temperature increased the bleaching performance. The optimum conditions were a dosage of 3.0 g,and a temperature of 100 oC at 50 minutes, resulting in the bleaching efficiency of 83.2%. Kinetic studies revealed that the Pseudo-second order model best described the adsorption process because it gave high regression coefficients at all operating temperatures. This indicated that chemisorption was the rate-controlling step in the adsorption process. The isotherm study revealed that the Temkin isotherm model gave the best fitting for the adsorption data because it displayed the highest $R^2$ values (>0.99) at all operating temperatures. The thermodynamic study showed that the bleaching process of crude palm oil with AAMC was endothermic due to the positive value of$\Delta H^o$ (61.9 KJ·mol$^{-1}$) obtained. Positive value of $\Delta S^o$ indicated that there was a high affinity of the adsorbent towards beta carotene. The value of the Gibbs free energy change indicated that the bleaching of crude palm oil with AAMC was non-spontaneous at 323 and 343 K but became spontaneous at higher temperatures. This study showed that alkaline-activated Amansea clay can be used as an alternative to imported adsorbents in the bleaching of palm oil at higher operating temperatures.

## COMPETING INTERESTS

Authors have declared that no competing interests exist.

## REFERENCES


1. Anyikwa SO, Nwakaudu MS, Nzeoma C, Yakubu E. Kinetics and equilibrium studies of colour pigments removal from crude palm oil using acid activated kaolin clay and mathematical method. International Journal of Science and Engineering Investigations.2021;10(116):30-44.
2. Egbuna SO, Omotioma M. Beneficiation of local clay to improve its performance in adsorption of carotene pigments and volatiles in the bleaching of palm oil. International Journal of Engineering Science Invention. 2013;2(12):21-28.
3. Ifa L, Wiyani L, Nurdjannah N, Ghalib AMT, Ramadhaniar S, Kusuma HS. Analysis of bentonite performance on the quality of refined crude palm oil's color, free fatty acid and carotene: The effect of bentonite concentration and contact time. Heliyon. 2021;7:e7230.
4. Akinwande BA, Salawudeen TO, Arinkoola AO, Jimoh MO. A suitability assessment of alkali activated clay for application in vegetable oil refining. International Journal of Engineering and Advanced Technology Studies.2014;2(1):1-12.
5. Oli SC, Kamalu CIO, Obijiaku JC, Opebiyi SO, Oghome P, Nkwocha AC. A study on the bleaching properties of locally sourced clay (Ukpor clay) for the processing of palm oil. International Journal of Modern Research in Engineering and Technology (IJMRET). 2017;2(5):4-29.
6. Mukasa-Tebandeke IZ, Wasajja-Navayojo ZH, Ssebuwufu PJM, Wasswa J, Nankinga R. Lugolobi F.et al. How variation of turbidity of bleached oils characterizes purity oil and bleaching processes. International Journal of Advanced Research in Chemical Science (IJARCS). 2017;4(5):36-65.
7. Salawudeen TO, Arinkoola AO, Jimoh MO, Akinwande BA. Clay characterization and optimisation of bleaching parameters for palm kernel oil using alkaline activated clays. Journal of Minerals and Materials Characterization and Engineering. 2014; 2:586-597.
8. Abdelfattah I, Abdelwahab W, El-Shamy AM. Montmorillonitic clay as a cost effective, eco-friendly and sustainable adsorbent for physicochemical treatment of contaminated water. Egyptian Journal of Chemistry.2022;65(2):687-694.
9. Bayram H, Ustunisik G, Önal M, Sarıkaya Y. Optimization of bleaching power by sulfuric acid activation of bentonite. Clay minerals.2021;56:148-155. Https://doi.org/10.1180/clm.2021.28.
10. Jozanikohan G, Abarghooei MN. The Fourier transform infrared spectroscopy (FTIR) analysis for the clay mineralogy studies in a clastic reservoir. Journal of Petroleum Exploration and Production Technology.2022;12:2093-2106.https://doi.org/10.1007/s13202-021-01449-y.
11. Ural N. The significance of scanning electron microscopy (SEM) analysis on the microstructure of improved clay: an overview. Open Geosciences. 2021;13:197–218.
12. Almeida ES, Carvalho ACB, Soares IO, Valadares LF, Mendonça ARV, Ivanildo JS. et al. Elucidating how two different types of bleaching earths widely used in vegetable oils industry remove carotenes from palm oil: Equilibrium, kinetics and thermodynamic parameters. Food Research International. 2019;121:785–797.
13. Kumar S, Panda AK, Singh RK. Preparation and characterization of acids and alkali treated kaolin clay. Bulletin of Chemical Reaction Engineering & Catalysis. 2013;8(1):61–69.
14. Nwabanne JT, Onu CE, Nwankwoukwu OC. Equilibrium, kinetics and thermodynamics of the bleaching of palm oil using activated Nando clay. Journal of Engineering Research and Reports.2018;1(3):1-13.
15. Ebelegi AN, Ayawei N, Wankasi D. Interpretation of Adsorption Thermodynamics and Kinetics. Open Journal of Physical Chemistry.2020;10:166-182. https://doi.org/10.4236/ojpc.2020.103010.

16. Nnanwube IA, Onukwuli OD, Okafor VN, Obibuenyi JI, Ajemba RO, Chukwuka CC. equilibrium, kinetics and optimization studies on the bleaching of palm oil using activated Karaworokaolinite. J. Mater. Environ. Sci. 2019;11(10):1599-1615.
17. Jasper EE, Ajibola VO, Onwuka JC. Nonlinear regression analysis of the sorption of crystal violet and methylene blue from aqueous solutions onto an agro□waste derived activated carbon. Applied Water Science.2020;10(132):1-11. https://doi.org/10.1007/s13201-020-01218-y.
18. Villabona-Ortíz Á, Figueroa-Lopez KJ, Ortega-Toro R. Kinetics and adsorption equilibrium in the removal of azo-anionic dyes by modified cellulose. Sustainability. 2022;14(6):3640. https://doi.org/10.3390/su14063640.
19. Piccin JS, Dotto GL, Pinto LAA. Adsorption isotherms and thermochemical data of FD&C REDo 40 binding by chitosan. Brazilian Journal of Chemical Engineering.2011;28(02):295-304.
20. Gunorubor AJ, Chukwunonso N. Kinetics, equilibrium and thermodynamics studies of $Fe^{3+}$ ion removal from aqueous solutions using periwinkle shell activated carbon. Advances in Chemical Engineering and Science. 2018; 8:49-66.
21. Okafor VN, Nnanwube IA, Obibuenyi JI, Onukwuli OD,Ajemba RO. Removal of pigments from palm oil using activated Ibusa kaolinite: Equilibrium, kinetic and thermodynamic studies. Journal of Minerals and Materials Characterization and Engineering.2019;7:157-170.
22. Nweke CN, Ajemba RO. Clay characterization and bleaching of crude palm oil using acid-activated Niboclay. Bioremediation Science and Technology Research. 2022;10(1):14-21.
23. Asadu CO, Ezema CA, Onu CE, Ike IS, Onoghwarite OE, Umeagukwu EO. Development of an adsorbent for the remediation of crude oil polluted water using stearic acid grafted coconut husk (Cocos nucifera) composite. Applied Surface Science Advances.2021;6(100179):1-18. https://doi.org/10.1016/j.apsadv.2021.100179.
24. Nandiyanto ABD, Oktiani R, Ragadhita R. How to read and interpret FTIR spectroscope of organic material. Journal of Science & Technology. 2019;4(1);97-118.
25. Stuart BH. Infrared Spectroscopy: Fundamentals and Applications. 1st Ed.John Wiley & Sons, Ltd: 2004;208 pages. ISBNs: 0-470-85427-8 (HB); 0-470-85428-6 (PB).
26. Coates J. Interpretation of Infrared Spectra, A Practical Approach. Encyclopedia of Analytical Chemistry, R.A. Meyers (Ed.):2000;10815-10837, Ó John Wiley & Sons Ltd, Chichester.
27. Thompson CO, Ndukwe AO, Asadu CO. Application of activated biomass waste as an adsorbent for the removal of lead (II) ion from wastewater. Emerging Contaminants. 2020;6:259-267.
28. Alhassan M, Suleiman M, Suleiman M, Safiya MA, Isah AA, Abdullahi B. et al. Performance of synthesized rice husk ash (RHA-based) adsorbent as a palm oil bleaching material. The International Journal of Engineering and Science (IJES). 2020;9(9):58-62.
29. Nwabanne JT, Ekwu CE. Decolourization of palm oil by Nigerian local clay: A study of adsorption isotherms and bleaching kinetics. International Journal of Multidisciplinary Sciences and Engineering.2013;4(1):20-25.
30. Abdullahi YA, Langkuk MT, Joseph KO, Adole VO, Segun AA, Mohammed SU. et al. Preparartion, characterization and comparison of adsorbents from Kirfi kaolin clay with commercial bleaching clay. International Journal of Research and Scientific Innovation (IJRSI). 2022;IX(VII):116-120.
31. Nwobasi VN, Igbokwe PK, Onu CE. Removal of methylene blue dye from aqueous solution using modified Ngbo clay. Journal of Materials Science Research and Reviews,2020;5(2):33-46.
32. Yi YM, Myat KT, Soe SN, Kyaw N. Removal of colouring materials and impurities in palm oil by using bentonite clay. J. Myanmar Acad. Arts Sci.2020;XVIII(1A):499-510.
33. Nadiye-Tabbiruka MS, Lungani L, Chaloba S, Ddamba W. Investigation of methyl orange adsorption from water using acid activated Makoro clay. American Journal of Materials Science.2018;8(4):73-78. DOI: 10.5923/j.materials.20180804.02.
34. Chairgulprasert, V. and Madlah, P. (2018) Removal of free fatty acid from used palm oil by coffee husk ash. *Science Technology Asia*, 23(3):1-9. doi: 10.14456/scitechasia.2018.18.
35. Onu CE, Nwabanne JT. Application of Response Surface Methodology in Malachite green adsorption using Nteje clay. Open Journal of Chemical Engineering and Science. 2014: 1 (2) 19 – 33.
36. Nwabanne JT, Okpe EC, Asadu CO, Onu CE. Sorption Studies of Dyestuffs on Low cost Adsorbent. Asian Journal of Physical and Chemical Sciences. 2018: 5(3)1–19. DOI: 10.9734/AJOPACS/2018/39338
37. Onu CE, Asadu CO, Ohale PE, Nweke, CN, Nwokedi IC, Musei NN, Onu CP. Adsorptive removal of bromocresol green dye using activated corn cob. Journal of Engineering and Applied Sciences. 2022: 21 (1): 824 – 841.
38. Onu CE, Nwabanne JT. Adsorption kinetics for Malachite green removal from aqueous solution using Nteje clay. Journal of Environment and Human. 2014: 1(2) 133 – 150. doi:https://doi.org/10.15764/EH.2014.02015